

SAQIEL: Ultra-Light and Safe Manipulator with Passive 3D Wire Alignment Mechanism

Temma Suzuki¹, Masahiro Bando¹, Kento Kawaharazuka¹, Kei Okada¹, and Masayuki Inaba¹

Abstract—Improving the safety of collaborative manipulators necessitates the reduction of inertia in the moving part. Within this paper, we introduce a novel approach in the form of a passive 3D wire aligner, serving as a lightweight and low-friction power transmission mechanism, thus achieving the desired low inertia in the manipulator’s operation. Through the utilization of this innovation, the consolidation of hefty actuators onto the root link becomes feasible, consequently enabling a supple drive characterized by minimal friction. To demonstrate the efficacy of this device, we fabricate an ultralight 7 degrees of freedom (DoF) manipulator named SAQIEL, boasting a mere 1.5 kg weight for its moving components. Notably, to mitigate friction within SAQIEL’s actuation system, we employ a distinctive mechanism that directly winds wires using motors, obviating the need for traditional gear or belt-based speed reduction mechanisms. Through a series of empirical trials, we substantiate that SAQIEL adeptly strikes balance between lightweight design, substantial payload capacity, elevated velocity, precision, and adaptability.

I. INTRODUCTION

In recent years, with the expansion of robots into society, there is a growing demand for manipulators that can operate in the same environments as humans. While conventional industrial robots avoid unintended collisions with their environment by operating within enclosures, manipulators designed to operate in living environments have a higher likelihood of unintended collisions with humans and surroundings. For such manipulators, innovative solutions are required to prevent damage to both the robot and the environment during collisions.

A quantifiable measure to assess robot safety is the maximum contact force when a human and a robot come into contact. When the human body’s contact points are not constrained by walls or floors, the maximum external contact force $F_{\text{ext}}^{\text{max}}$ is expressed by the following equation [1]:

$$F_{\text{ext}}^{\text{max}} = \sqrt{\frac{m_u M_H}{m_u + M_H}} \sqrt{K_H \dot{x}_{\text{re}}^0} \quad (1)$$

here, m_u represents the effective mass of the robot’s contact point, M_H is the effective mass of the human body’s contact point, K_H stands for the effective stiffness of the contact point, and \dot{x}_{re}^0 denotes the relative collision velocity between the robot and the human. From this equation, it is apparent that reducing the effective mass m_u of the robot can decrease the maximum contact force $F_{\text{ext}}^{\text{max}}$ without lowering the collision speed \dot{x}_{re}^0 . Thus, efforts have been made to achieve both

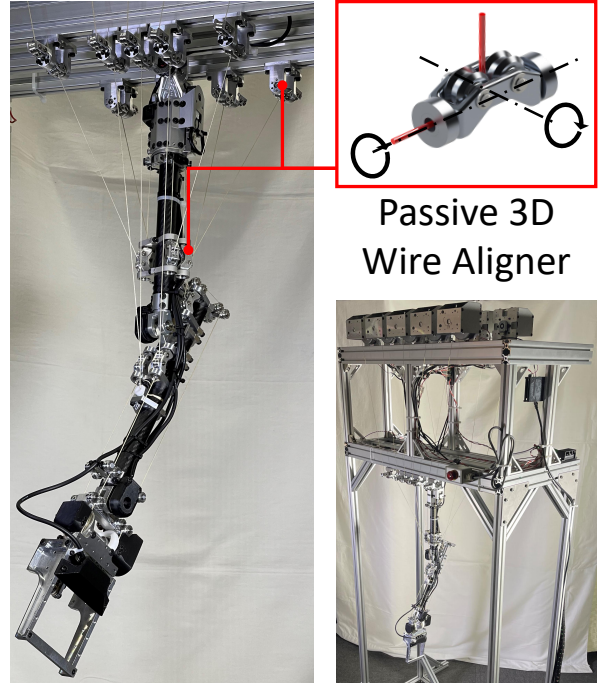


Fig. 1. Overview of passive 3D wire aligner and 7-DoF manipulator SAQIEL with this mechanism.

high-speed operation and safety by minimizing the inertia of the manipulator’s moving part.

Among the components comprising a manipulator, the gearbox and actuators contribute significantly to the overall weight. Kim and colleagues have approached the challenge by utilizing wires for power transmission, consolidating motors that drive the manipulator’s wrist and elbow onto the upper arm, thus reducing the inertia of the moving part [2]–[4]. However, a drawback of this method is that actuators are still mounted on the moving part.

A method to aggregate motors on the root link is the concept of coupled tendon-driven actuation [5], [6]. This technique employs a redundant number of wires relative to the number of joints to transmit power. As a result, actuators can be completely removed from the moving part. The coupled tendon-driven robot arm developed by Yokoi et al. had a total length of 843 mm and a moving part weight of 4 kg [6]. Considering that a commercially available collaborative robot arm of similar size (total length 850 mm) has a moving part weight of 17.7 kg [7], it becomes evident that coupled tendon-driven actuation can significantly reduce the moving part weight.

However, in coupled tendon-driven actuation, since the

¹ The authors are with the Department of Mechano-Informatics, Graduate School of Information Science and Technology, The University of Tokyo, 7-3-1 Hongo, Bunkyo-ku, Tokyo, 113-8656, Japan. [suzuki, bando, kawaharazuka, okada, inaba]@jsk.t.u-tokyo.ac.jp

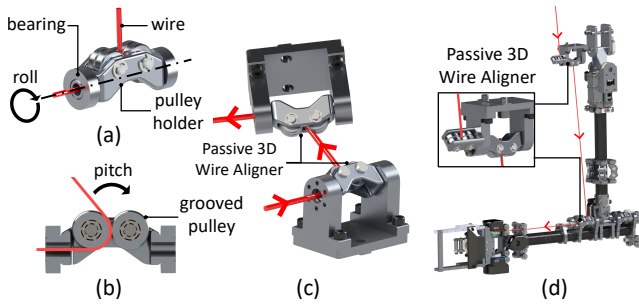


Fig. 2. Detail of passive 3D wire aligner. (a) overview of the wire aligner and roll axis rotation of the wire, (b) cross section of the wire aligner and pitch axis rotation of the wire, (c) pair of wire aligner, (d) wire aligner transmitting a wire inside a 7-DoF manipulator.

wires pass through all joints up to the terminal link, a large-diameter pulley wound with wires is necessary for each joint (about half the number of wires times the number of joints). Consequently, the complexity of the joint mechanism increases, and there is a potential drawback of increased overall weight of the moving part.

As a simple and lightweight method to transmit power from actuators on the root link to each joint, one approach is to use wires and tubes. In this method, wires pass through tubes to transmit power from the root link to the desired link [8], [9]. Using this approach, Mustafa et al. achieved a lightweight 7-DoF robot arm with a moving part weight of 1 kg [8]. This approach yields a simple and lightweight mechanism; however, it introduces challenges such as friction between the wires and tubes, making the modeling of the wire-driven system complex.

Therefore, in this study, we aim to create a lightweight, low-friction mechanism that enables power transmission across multiple joints and works toward achieving a safe multi-degree-of-freedom manipulator. To achieve this goal, we propose a passive 3D wire aligner, as illustrated in Fig. 1, which allows transmission of wires across multiple joints.

It should be noted that the primary focus of this study is on the hardware design of a lightweight, flexible and safe manipulator, rather than the improvement of end-effector positioning accuracy or the development of new control methods for wire-driven robots.

II. PASSIVE 3D WIRE ALIGNER

A. Feature of Passive 3D Wire Aligner

The detailed structure of the passive 3D wire aligner is illustrated in Fig. 2. When a wire passes through this device, it aligns with a predetermined straight line regardless of the angle at which the wire enters the device. By installing a wire aligner on each of the two links, a wire path connecting the two links in a straight line can be established.

The advantages of the wire aligner lie in its lightweight design and low friction. In conventional coupled tendon-driven systems, the required number and weight of pulleys increase proportionally with the number of joints they traverse. In contrast, this method enables power transmission between the two links without passing through intermediate

joints by using only one set of wire aligners. Furthermore, this approach employs grooved pulleys with built-in bearings to guide the wire, eliminating sliding parts and reducing friction.

A similar approach involves placing a wire alignment mechanism on one of the links and anchoring the wire end to the other link [10]. In this method, power transmission via the wire is limited to specific two links. In contrast, our approach uses pairs of wire alignment mechanisms, allowing power transmission to links other than the two links equipped with the wire alignment mechanism. Therefore, our method can transmit power to links further away than existing methods.

B. Design of Passive 3D Wire Aligner

As shown in Fig. 2, the passive 3D wire aligner automatically accommodates the wire's pitch and roll displacements upon entry. The alignment in the pitch direction of the wire is achieved by winding the wire around the grooved pulley. This grooved pulley incorporates needle bearings, enabling low-friction wire transmission. Additionally, by sandwiching the wire between two grooved pulleys, the wire is prevented from dislodging from the aligner.

Alignment in the roll direction of the wire is achieved through rotation of the pulley holder. This rotational degree of freedom is facilitated by deep groove ball bearings attached at both ends of the pulley holder.

In this study, a passive 3D wire aligner was designed for use with a Vectran rope of diameter 1 mm (tensile strength of 1560 N, VB-175, Hayami Industry), assuming a maximum tension of 500 N. By adopting the slim 1 mm diameter wire, the device was successfully miniaturized and lightweighted to dimensions of 44 mm × 16 mm × 21 mm and a weight of 27 g.

III. DESIGN OF 7-DOF MANIPULATOR WITH PASSIVE 3D WIRE ALIGNER

A. Overview

In this chapter, we provide a detailed description of the design of the 7-degree-of-freedom manipulator, termed SAQIEL (SAfe, QuIck and Extremely Lightweight manipulator), created for the purpose of validating the performance of the passive 3D wire aligner.

As mentioned in Section I, reducing the effective mass of the manipulator is crucial to enhance safety during collisions. Moreover, improving joint backdrivability is effective for enhancing safety during quasi-static contact scenarios such as crushing or clamping. Therefore, the design objectives of SAQIEL are as follows:

- 1) Minimization of effective mass.
- 2) Reduction of friction in the power transmission system.

Furthermore, these design objectives should be achieved while ensuring payload capacity, accuracy, and operational speed.

For design goal 1), SAQIEL has all drive motors located on the root link. An overview of SAQIEL is presented in Fig. 3. The structure involves 10 motors on the root link, each winding wires to control the 7-DoF manipulator. Power

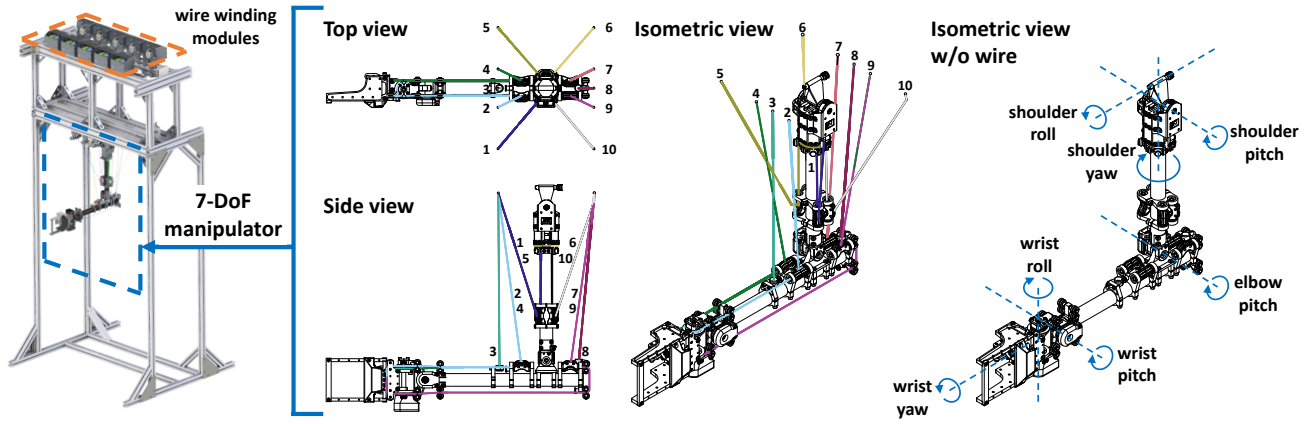


Fig. 3. Overview of SAQIEL.

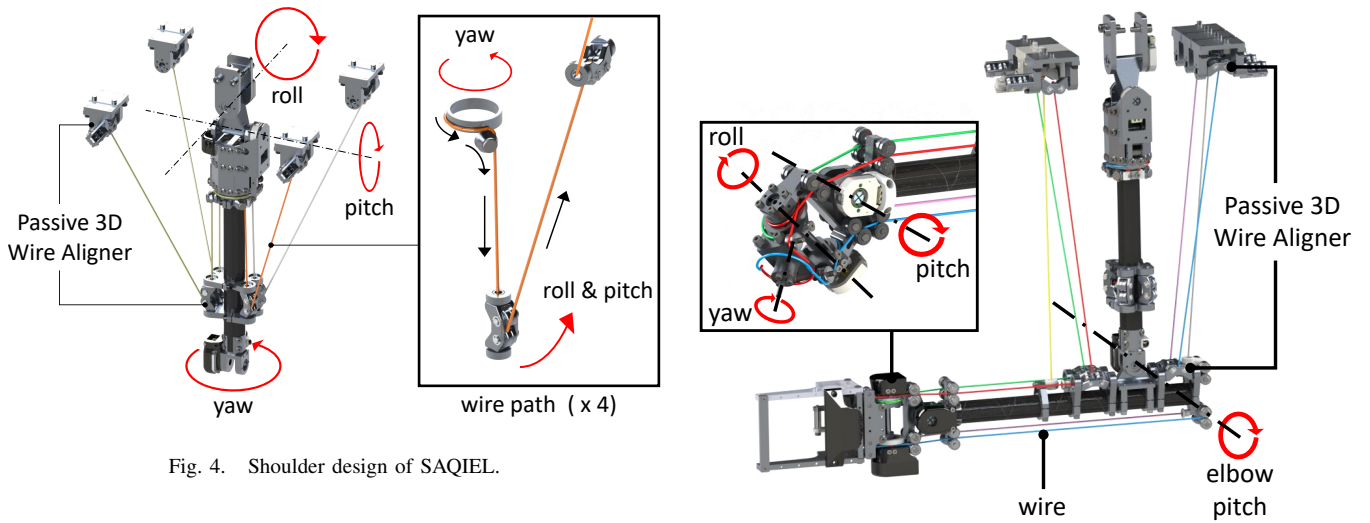


Fig. 4. Shoulder design of SAQIEL.

transmission from the root link to each link is facilitated by 10 sets of passive 3D wire aligners.

For design goal 2), SAQIEL employs a mechanism in which motors directly wind the wires without the use of gear or belt-based reduction mechanisms. Detailed specifications of the gearless wire modules are explained in Section III-D. Additionally, through the use of multiple small pulleys in the wire path to eliminate sliding parts, low-friction power transmission is achieved.

The primary specifications of SAQIEL are presented in Table. I. SAQIEL's arm length is 0.78 m, similar to a human arm. However, the total weight of the moving parts (all links except the root link) is approximately 1.5 kg. This is about 60% lighter compared to the weight of a human upper limb of the same length (4.1 kg) [11].

SAQIEL features two types of wire paths: linear and circular. The definitions of each path are as follows:

- Linear wire path: A straight line connecting specific points on two links.
- Circular wire path: An arc coaxial with the joint axis.

Each path has its respective advantages: linear paths facilitate larger moment arms, while circular paths enable larger range of motion. Balancing lightweight design and range of motion, the choice of wire paths is made for each joint.

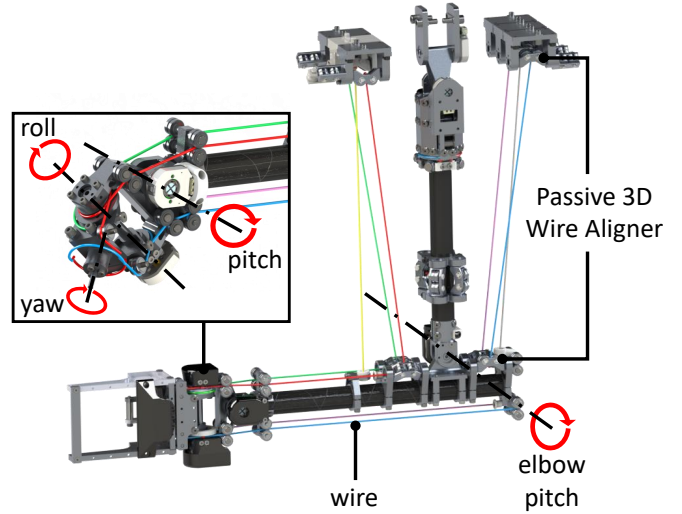


Fig. 5. Elbow and wrist design of SAQIEL.

B. Shoulder Mechanism

In the design of the manipulator's shoulder joint, it is crucial to balance sufficient joint torque and lightweight characteristics. Conventional coupled tendon-driven robots [5], [6] employ numerous large-diameter pulleys on the shoulder section to ensure joint torque. However, the extensive use of large-diameter pulleys complicates the mechanism and increases its weight. In the shoulder component of SAQIEL, a passive 3D wire aligner is employed to achieve balance between a large moment arm and lightweight design.

Detailed structures of the three shoulder joints (roll, pitch, yaw) are depicted in Fig. 4. The shoulder roll, pitch, and yaw joints are mainly controlled by four wires (wires 1, 5, 6, 10) arranged circularly around the upper arm's long axis. These four wires follow the path: root link \rightarrow upper arm link \rightarrow shoulder link.

Four sets of passive 3D wire aligners are placed on the root link and the upper arm link, connecting the two links with a linear wire path. This configuration allows for a significant moment arm (approximately 90 mm) around the shoulder roll and pitch axes. Furthermore, due to the wires not passing through the interior of the shoulder joint, a

lightweight shoulder joint (weighing around 0.5 kg, including the shoulder joint and upper arm link) with fewer large-diameter pulleys can be realized.

The upper arm link to the shoulder link is connected by a circular wire path around the shoulder yaw axis. The four wires passing through the passive 3D wire aligner on the upper arm link wind around coaxial pulleys on the shoulder link. The ends of these wires wound around the pulley are fixed on the shoulder link.

C. Elbow and Wrist Mechanism

To reduce the effective mass of the manipulator, lightweight design of links near the end effector is crucial. Therefore, in the design of SAQIEL's elbow pitch joint and three joints of wrist (pitch, roll, yaw), the goal was to create a lightweight configuration with the minimal required number of parts.

Detailed designs of the elbow pitch joint and three joints of wrist are presented in Fig. 5. The elbow pitch joint is controlled by six linear wire paths (wires 2, 3, 4, 7, 8, 9) connecting the root link and the forearm link. These six wire paths coincide with the straight lines connecting six passive 3D wire aligners on the root link side as well as four passive 3D wire aligners and two wire termination components on the forearm link side. By adopting linear wire paths similar to the shoulder roll and pitch joints, balance between lightweight design (0.5 kg) and a large moment arm is achieved.

Among the wires driving the elbow pitch joint, four (wires 2, 4, 7, 9) extend from the forearm link to the end effector link, controlling the wrist's three joints (wrist pitch, wrist roll, wrist yaw). The range of motion of the wrist joints is based on the human body. A linear wire path is used to drive the wrist pitch joint, which has a small range of motion, and a circular wire path is used to drive the wrist roll and yaw joints, which have a large range of motion. Moreover, considering that the required torque for the wrist joints is smaller compared to the shoulder and elbow, a configuration using small pulleys was employed for creating the wire paths instead of 3D passive wire aligners. By choosing appropriate wire paths and path creation methods based on the required joint torques and ranges of motion, a lightweight (0.5 kg) and large-range-of-motion wrist joint was realized.

D. Gear-less Wire Winding Module Mechanism

As mentioned in Section III-A, the design requirement of this mechanism is to achieve low-friction wire winding without using a gearbox. In this study, a high torque constant BLDC gimbal motor (T-MOTOR GL80 KV30) was utilized to achieve low-friction wire winding without the need for a gearbox.

Detailed design of the gearless wire module is presented in Fig. 6. 1 mm diameter Vectran rope (tensile strength of 1560 N, VB-175, Hayami industry) is wound around a 10 mm diameter pulley fixed to the motor. The peak tension is 490 N, providing sufficient tension to drive each joint.

TABLE I
PHYSICAL PARAMETERS OF SAQIEL.

Items		Value
Mass without electrical wiring	total moving part	1.5 kg
	upper arm	0.5 kg
	forearm	0.5 kg
	wrist	0.5 kg
Range of motion	shoulder roll	-55 deg~55 deg
	shoulder pitch	-55 deg~55 deg
	shoulder yaw	-90 deg~90 deg
	elbow	-60 deg~60 deg
	wrist pitch	-45 deg~45 deg
	wrist roll	-80 deg~80 deg
	wrist yaw	-150 deg~150 deg
Distance between joints	shoulder roll - elbow pitch	0.34 m
	elbow pitch - wrist pitch	0.24 m
	wrist pitch - fingertip	0.20 m
Upper limb length		0.78 m
Maximum wire tension		490 N
Maximum wire speed (no load)		0.86 m/s

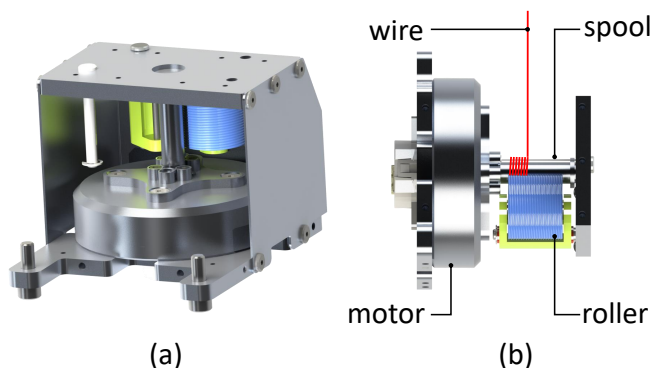


Fig. 6. Wire winding module design of SAQIEL. (a) isometric view of the module, (b) winding mechanism of the module.

To prevent wire entanglement and ensure accurate winding length, a grooved roller is pressed against the wire on the pulley's surface. This design feature effectively prevents wire entanglement and ensures precise winding length.

IV. CONTROLLER OF 7-DOF MANIPULATOR WITH PASSIVE 3D WIRE ALIGNER

The controller of SAQIEL is depicted in Fig. 7. SAQIEL employs a control strategy based on the Computed Torque Method. However, due to the adoption of the coupled tendon-driven mechanism, the desired joint torques τ_{ref} are transformed into target wire tensions f_{ref} after computation [12].

The torques τ at the joints generated by the tension f of the wires can be calculated using the following equation:

$$\tau = -G^T f \quad (2)$$

here, G is a matrix representing the moment arm of each wire at each joint, known as the muscle Jacobian. The muscle Jacobian $G(q)$ at a specific joint angle q is defined as:

$$G(q) = \frac{\partial l}{\partial q} \quad (3)$$

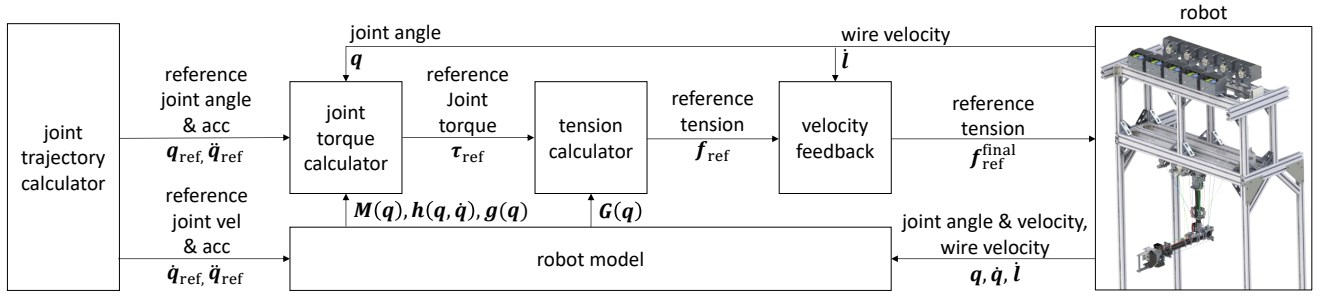


Fig. 7. Controller of SAQIEL.

where l is the current wire length. Using Equation (2), the target wire tension f_{ref} that satisfies the target joint torque τ_{ref} is determined by solving the following quadratic programming problem [12]:

$$\begin{aligned} & \text{minimize} && |f_{\text{ref}}|^2 + (\tau_{\text{ref}} + G^T f_{\text{ref}})^T \Lambda (\tau_{\text{ref}} + G^T f_{\text{ref}}) \\ & \text{subject to} && f_{\text{min}} \leq f_{\text{ref}} \leq f_{\text{max}} \end{aligned} \quad (4)$$

here, Λ is the weight matrix for each joint torque, $f_{\text{min}} / f_{\text{max}}$ is the minimum / maximum tension for each wire. The first term of the objective function minimizes the magnitude of wire tension, while the second term minimizes the error between the target joint torque and the actual joint torque generated by wire tension. Solving this quadratic programming problem allows us to determine the minimized target wire tension f_{ref} while satisfying the target joint torque.

Since the moment arm of linear wire paths varies with joint angles, the muscle Jacobian $G(q)$ needs to be recalculated for each change in joint angle. A muscle Jacobian calculation library that accommodates both linear and circular wire paths was developed in this study. This library enables the conversion from desired joint torques to target wire tensions to be performed at a high frequency of over 500 Hz.

The calculation of the desired joint torques τ_{ref} is derived from the following equation:

$$\tau_{\text{ref}} = M(q)(K_p(q_{\text{ref}} - q) + \ddot{q}_{\text{ref}}) + h(q, \dot{q}) + g(q) \quad (5)$$

where q represents the current joint angle vector, $M(q)$ is the inertia matrix, K_p is the position feedback gain matrix, q_{ref} is the target joint angle, \ddot{q}_{ref} is the target joint acceleration derived from the desired trajectory, $h(q, \dot{q})$ is the vector representing centrifugal and Coriolis forces, and $g(q)$ is the gravity vector.

Notably, unlike the conventional computed torque method, the feedback term concerning joint angular velocity \dot{q} is absent. This is due to the use of wire velocity \dot{l} rather than joint angular velocity \dot{q} for velocity feedback. Delay arises between the motor output shaft angular velocity and the joint angular velocity due to the elasticity of the wire used for power transmission. Consequently, using feedback based on joint angular velocity \dot{q} (acquired from joint encoders) could lead to manipulator oscillations. Therefore, this study employs feedback based on wire velocity \dot{l} (acquired from encoders attached to the motors). The final target wire tensions $f_{\text{ref}}^{\text{final}}$ including the velocity feedback term are

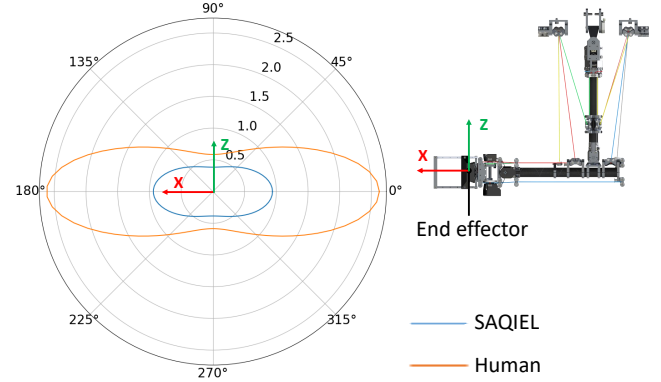


Fig. 8. Effective mass of SAQIEL.

calculated using the following equation:

$$f_{\text{ref}}^{\text{final}} = K_v(\dot{l}_{\text{ref}} - \dot{l}) + f_{\text{ref}} \quad (6)$$

here, K_v is the velocity feedback gain matrix, and \dot{l}_{ref} represents the desired wire velocity.

V. EXPERIMENTS

A. Analysis of Effective Mass

The effective mass of a manipulator at a certain contact point refers to the perceived mass experienced when the manipulator makes contact [13]. As shown in Eq. (1), a smaller effective mass leads to lower contact forces during collisions, enabling high-speed operation while maintaining safety [1]. In this section, we numerically calculate the effective mass of the end effector of SAQIEL to verify its safety.

In Fig. 8, the computed results of the effective mass for SAQIEL and the human arm in the xz plane are depicted. The maximum effective mass of SAQIEL (excluding the motor rotor inertia) is 0.94 kg. This is approximately one-third of the maximum effective mass of the human arm (2.6 kg), highlighting its lightweight nature. It should be noted that the calculation of the human effective mass employs a URDF model [11] of a human with the same upper limb length as SAQIEL.

Prior studies aiming to reduce effective mass, similar to our research, include the 7-DoF manipulators *lims1* [2] and *lims2* [3], which consolidated motors for elbow and wrist actuation in the upper arm. *lims1* had a maximum effective mass of 1.5 kg, while *lims2* had a maximum effective

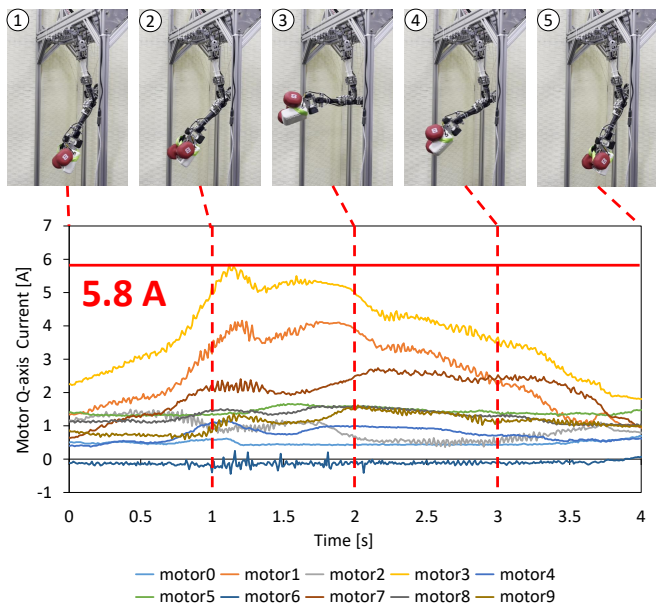


Fig. 9. Payload test with 3.74 kg weight. Maximum motor q-axis current is 5.8 A (power invariant transformation).

mass of 2.1 kg. In comparison, SAQIEL’s effective mass is approximately 2/3 to 1/2 that of these prior studies. This demonstrates the significant contribution of the passive 3D wire aligners to the lightweight design of the manipulator.

B. Payload Test

To demonstrate SAQIEL’s capability to exert sufficient force, a lifting motion test with a heavy payload is conducted. The sequential images of the test and the q-axis current values (power invariant transformation) of each motor are presented in Fig. 9.

In this test, a weight of 3.7 kg is fixed to the end effector, and the elbow pitch joint is moved from -44° to 20° . During this movement, the motors are subjected to q-axis currents of up to approximately 5.8 A, which is about half of the allowable peak current of 10 A. This test confirms that SAQIEL is both lightweight and flexible while providing sufficient actuating force.

C. High Speed Motion Test

To demonstrate SAQIEL’s capability for high-speed operation, a ball throwing experiment is conducted. Sequential images of the experiment along with the end effector velocity are depicted in Fig. 10.

In this experiment, a 31 g ball is thrown from the end effector. Initially, the ball is gripped by three fingers (rigid rods without moving parts) on the end effector. By providing a desired trajectory to SAQIEL, both the end effector and the ball are accelerated. As the trajectory’s end point is approached, the end effector decelerates, causing the ball to be propelled by its inertia. As explained in Section IV, trajectory tracking is achieved through position feedback from joint encoders and wire velocity feedback from motor encoders.

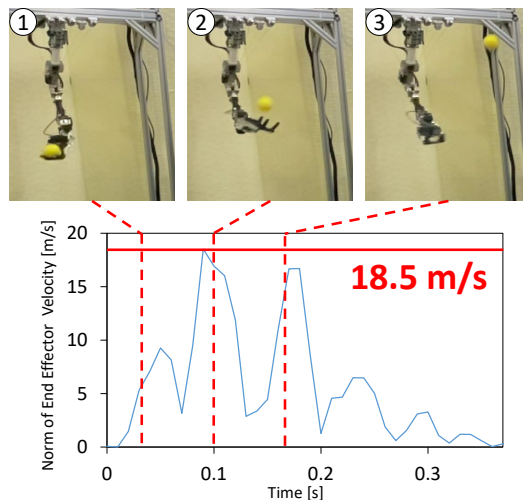


Fig. 10. High speed motion test. SAQIEL throw a ball with the end effector speed of 18.5 m/s

The maximum distance the ball travels is approximately 4.8 m. Furthermore, the maximum end-effector velocity was approximately 18.5 m/s. This value significantly surpasses the operational speed of 1 m/s for the wave gear-driven collaborative robot [14] and exceeds the 5.35 m/s speed of other lightweight wire-driven manipulator [2]. This extreme end-effector velocity is achieved by utilizing the lightweight and flexible characteristics inherent in the coupled tendon-driven system and vigorous swinging of the wrist. This experiment confirms that due to its low effective mass, SAQIEL is capable of generating substantial end effector accelerations, making it well-suited for high-speed operations.

D. Accuracy Test

To demonstrate SAQIEL’s position control capability, a high-speed trajectory tracking experiment is conducted. Sequential images of the experiment and the trajectory of the end effector position are illustrated in Fig. 11.

In this experiment, the end effector is made to track a circular trajectory (diameter of 0.25 m, period of 0.6 s). The maximum position error of the end effector during this trajectory tracking is 11 mm.

The primary causes of end-effector position errors include cogging torque in the motor, friction between the wire and pulley, and the elasticity of the wire, which result in discrepancies between the commanded tension and the actual tension. Incorporating these factors into the control model can be expected to reduce the error between commanded tension and actual tension, thus improving end-effector positioning accuracy.

E. Passive Collision Test

To assess the response of SAQIEL when subjected to external impact, a collision experiment is conducted by striking a weight against SAQIEL. Sequential images of the experiment and the changes in wrist pitch and elbow pitch joint angles are presented in Fig. 12.

In this experiment, a 5 kg ball is dropped from a height of 1 m onto the SAQIEL, which is under position control. The

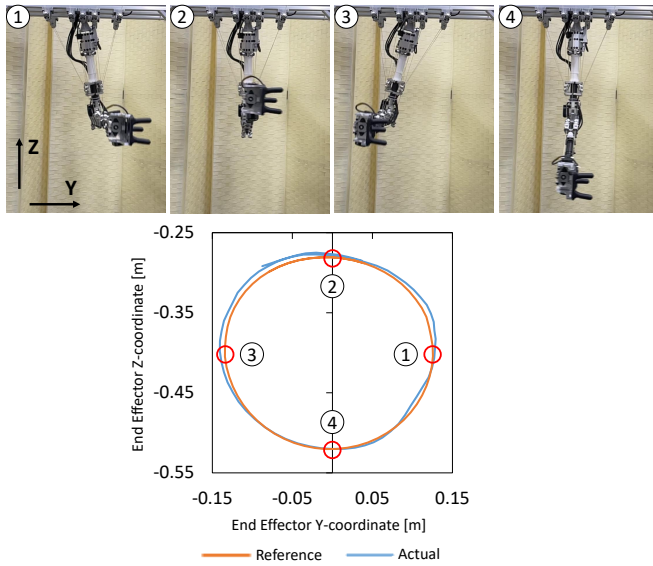


Fig. 11. Circular trajectory (diameter:0.25 m, period:0.6 s) following experiment.

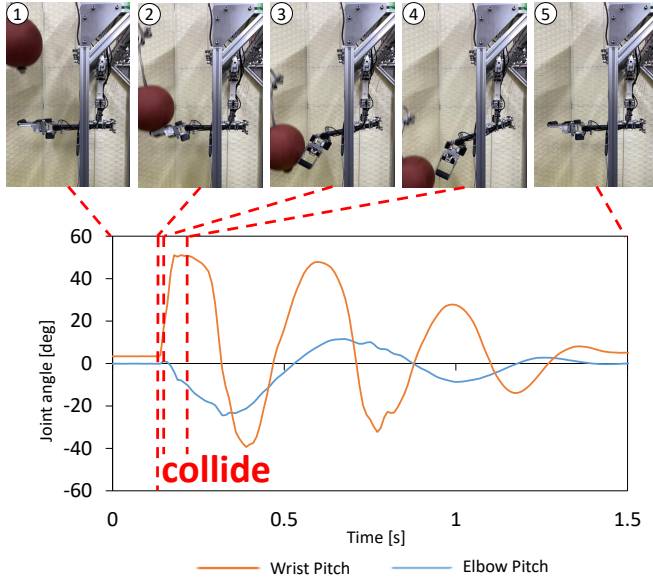


Fig. 12. Passive collision test. Dropping a 5 kg weight from a height of 1m and inducing collision with SAQIEL.

velocity of the weight at the moment of impact is estimated to be approximately 4.4 m/s based on the fall distance. To enhance flexibility, the gains for joint angle feedback and wire velocity feedback are set to about one-tenth of those in Section V-D.

From Fig. 12, it can be observed that after the collision, the wrist pitch joint angle shifts by 50° within 0.05 s, and the elbow pitch joint angle shifts by -24° within 0.17 s. Responding quickly and flexibly to external impacts in this manner is challenging for robots with high friction in their drive systems or substantial moving part masses. This experiment confirms that SAQIEL can respond softly and safely to external impacts.

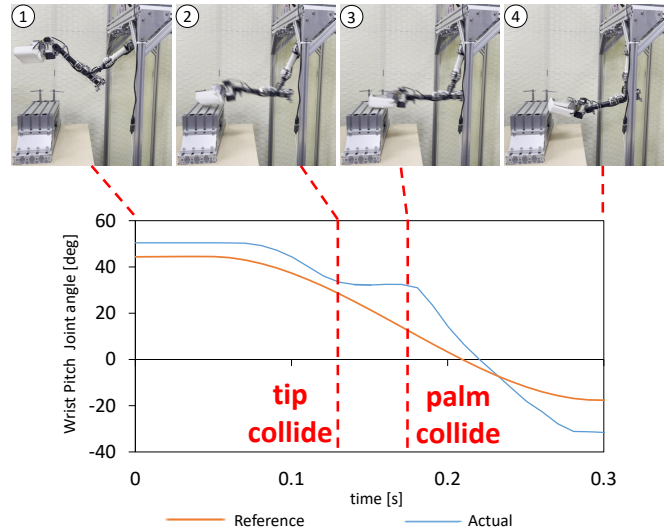


Fig. 13. Active collision test. SAQIEL impacts an aluminium frame.

F. Active Collision Test

To assess the response of SAQIEL when colliding with the environment during operation, an experiment is conducted where SAQIEL strikes an aluminum frame. Sequential images of the experiment and changes in wrist pitch joint angle are presented in Fig. 13.

In this experiment, similar to Section V-D, SAQIEL follows a target trajectory. The collision between SAQIEL and the aluminum frame is set to occur at the lower end of the target trajectory. The collision portion of SAQIEL is made of rigid components created using a 3D printer, without the use of elastic materials such as rubber or springs for impact absorption.

From the sequential images in Fig. 13, it can be observed that SAQIEL's tip and palm sequentially come into contact with the aluminum frame. Furthermore, from the plot of the wrist pitch joint angle, it can be confirmed that within 0.1 s after the collision, the end effector moves along the surface of the aluminum frame. These results indicate that SAQIEL is capable of flexible environmental contact even during operation.

Performing such intense contact with the environment on a typical industrial manipulator can pose a risk of damaging both the environment and the robot. However, in this experiment, neither SAQIEL nor the aluminum frame exhibited any damage. This suggests that lightweight and flexible structures like SAQIEL's have the potential to enhance the safety of robots by mitigating the risk of damage in such environmental interactions.

VI. CONCLUSION

In this study, we propose a lightweight and low-friction power transmission mechanism called the passive 3D wire aligner to achieve a lightweight, flexible, and safe manipulator. By using this approach to transmit actuator power from the root link, a simple and lightweight moving part can be created. Furthermore, as this method employs a wire

and needle bearing-based power transmission, it ensures low friction due to the absence of sliding components.

To validate the performance of this approach, we developed a 7-DoF wire-driven manipulator named SAQIEL. Through numerical analysis, we confirmed that SAQIEL's effective mass is approximately two-thirds of that of conventional lightweight manipulators [2]. Furthermore, we verified its capability to handle sufficient payloads, achieve maximum velocities, maintain position control, and exhibit flexibility for various tasks. Additionally, tracking experiments of end-effector trajectories have been conducted, indicating that friction between the wire and pulley, as well as the elasticity of the wire, are the causes of end-effector position errors.

Future challenges include measuring and enhancing the transmission efficiency of the passive 3D wire aligner. By evaluating the transmission efficiency in different wire materials and pulley shapes, further performance improvements are anticipated. Moreover, advanced tasks such as introducing a parallel link structure for wire interference avoidance and exploring applications in leg mechanisms can be considered. Furthermore, by optimizing wire arrangements and increasing the implementation density of motor modules and 3D passive wire aligners, it becomes possible to realize smaller and lighter root links. This opens up the potential for applications in humanoid robots and wheeled robots.

REFERENCES

- [1] S. Haddadin, "Physical Safety in Robotics," in *Formal Modeling and Verification of Cyber-Physical Systems: 1st International Summer School on Methods and Tools for the Design of Digital Systems*, R. Drechsler and U. Kühne, Eds. Springer Fachmedien Wiesbaden, 2015, pp. 249–271.
- [2] C. Latella, Y. Tirupachuri, L. Rapetti, and R. Grieco, "human-gazebo/humanSubject04/humanSubject04_48dof.urdf," https://github.com/robotology/human-gazebo/blob/master/humanSubject04/humanSubject04_48dof.urdf.
- [3] Y.-J. Kim, "Anthropomorphic low-inertia high-stiffness manipulator for high-speed safe interaction," *IEEE Transactions on robotics*, vol. 33, no. 6, pp. 1358–1374, 2017.
- [4] H. Song, Y.-S. Kim, J. Yoon, S.-H. Yun, J. Seo, and Y.-J. Kim, "Development of low-inertia high-stiffness manipulator limbs for high-speed manipulation of foldable objects," in *Proceedings of the 2018 IEEE/RSJ International Conference on Intelligent Robots and Systems*, 2018, pp. 4145–4151.
- [5] "New LIMS with Improved Performance! LIMS3-AMBIDEX," <https://www.youtube.com/watch?v=7INPj1hdnyA>.
- [6] S. Hirose and S. Ma, "Coupled tendon-driven multijoint manipulator," in *Proceedings of the 1991 IEEE International Conference on Robotics and Automation*, 1991, pp. 1268–1275.
- [7] K. Yokoi, K. Tanie, N. Inamura, T. Kawai, and K. Agou, "Design and control of a seven-degrees-of-freedom manipulator actuated by a coupled tendon-driven system," in *Proceedings IROS'91: IEEE/RSJ International Workshop on Intelligent Robots and Systems' 91*, 1991, pp. 737–742.
- [8] "UR5e," <https://www.universal-robots.com/media/1807465/ur5e-rgb-fact-sheet-landscape-a4.pdf>.
- [9] S. K. Mustafa, G. Yang, S. H. Yeo, W. Lin, and I.-M. Chen, "Self-calibration of a biologically inspired 7 dof cable-driven robotic arm," *IEEE/ASME transactions on mechatronics*, vol. 13, no. 1, pp. 66–75, 2008.
- [10] Q. Chen, W. Chen, G. Yang, and R. Liu, "An integrated two-level self-calibration method for a cable-driven humanoid arm," *IEEE Transactions on Automation Science and Engineering*, vol. 10, no. 2, pp. 380–391, 2013.
- [11] Z. Zhang, Z. Shao, and L. Wang, "Optimization and implementation of a high-speed 3-dofs translational cable-driven parallel robot," *Mechanism and Machine Theory*, vol. 145, p. 103693, 2020.
- [12] M. Kawamura, S. Ookubo, Y. Asano, T. Kozuki, K. Okada, and M. Inaba, "A joint-space controller based on redundant muscle tension for multiple dof joints in musculoskeletal humanoids," in *Proceedings of the 2016 IEEE-RAS International Conference on Humanoid Robots*, 2016, pp. 814–819.
- [13] O. Khatib, "Inertial properties in robotic manipulation: An object-level framework," *The international journal of robotics research*, vol. 14, no. 1, pp. 19–36, 1995.
- [14] "UR3e," <https://www.universal-robots.com/media/1807464/ur3e-rgb-fact-sheet-landscape-a4.pdf>.